# Some Useful Guidelines for Whole Core CT-Scanning for Petrophysical Applications

*Shameem* Siddiqui[1,2*]

[1]Halliburton Consulting, 3000 N. Sam Houston Pkwy, E, Houston, TX 770, USA
[2]ResVisions LLC, 16902 Cook Landing Drive, Richmond, TX 77407

**Abstract.** From the time CT-scanning was introduced in the oil and gas industry, its use could be divided into SCAL and routine type applications. The first involves flowing fluids through the cores, whereas the second involves scanning, mainly the whole cores, in their native (preserved or unpreserved) state. For whole core CT-scanning, there has been a constant shift from qualitative to quantitative analysis. The size of whole cores is ideal for scanning them with a 'converted' medical CT-scanner but obtaining meaningful data requires more than just artifact-free images. In this paper, useful guidelines are offered for extracting meaningful quantitative data from whole core CT-scanning. Today's fast, multi-slice medical CT-scanners generally provide sufficient image resolution for most of the whole core related applications. However, they usually require some modifications to the equipment and the calibration procedures. Special solid phantoms matching the size and density should be used for calibrating the scanner at different X-ray energies. A set of calibration 'standards' is necessary for converting the CT numbers into density and $Z_{eff}$ (Effective Atomic numbers), which should be scanned under the similar 'environment' as the whole cores. Using pilot scans is highly recommended for every core tube to reduce uncertainties. For dual energy scanning, it is important to take scans at the exact same locations, selecting the right energy pair and corresponding calibration tables. For image processing, important guidelines include aligning the first and last slices for selecting the largest region-of-interest, quality controlling each slice and assigning depths to each slice before converting from CT numbers to bulk density and $Z_{eff}$. Additional information is provided for scanning with industrial CT-scanners which have both advantages and disadvantages. Guidelines such as the ones mentioned above allow the data from whole core CT imaging useful for a number of applications. Such data were successfully used for bulk density and porosity determination, heterogeneity quantification, lithology determination, dual-energy based mineralogy detection, density-based micro-imaging, core-log correlations and depth matching, fracture characterization, formation damage evaluation, and many others. Several examples are included in this paper. Adherence to strict guidelines helps extracting artifact-free, meaningful data on whole cores that can improve our understanding of rocks. This paper demonstrates at least 10 different applications of CT-scanners along with the proper guidelines that can be useful for engineers and geoscientists.

## 1 Introduction

CT-scanning has been used for core characterization and flow visualization in reservoir rocks for over 35 years. In the flow visualization category, CT-scanning has been successfully used for porosity and pore volume compressibility determination, two- and three-phase flow visualization and quantification, and for evaluating core treatments such as acidizing, foam injection, EOR fluid injection, etc. CT-based core plug screening has been one of the most popular early uses of the technology. Although the other core characterization applications came a little later, CT-based characterization includes evaluating core quality, identifying and quantifying bulk lithology, measuring density and porosity, integrating CT-derived density and porosity with log-derived data, depth matching, quantifying heterogeneity detection of fractures, visualization and evaluation of mud or treatment fluid invasion, etc. While most of these petrophysical applications apply equally to whole cores and plugs, the focus will be on whole core CT-scanning only.

Cores collected from reservoirs during the exploration and development phases can provide very important petrophysical, paleontological, sedimentological, petro graphic, and diagenetic information and therefore, utmost care should be taken to avoid damaging the cores. Some of the best practices in core handling involves onsite sectioning of the cores, while inside their aluminum or fiberglass sleeves, into 3 ft (about 1 m) long sections, marking the depths and identifying tops (typically with two parallel lines, red and black), putting caps on both ends and then putting these sleeves in reservoir compatible brine inside a PVC core box in order to preserve wettability (Fig. 1). The core box, without brine, also serves to protect the core integrity during transportation. After carefully transporting the core boxes to the core handling facility, CT-scanning should be one of the first operations executed on core samples because core integrity is compromised once the core is extracted from its sleeve (Fig. 2) for core description, slabbing and plugging. This way the three-dimensional, mostly density-related data remains available for any future qualitative and quantitative use, even after the core becomes subjected to extensive slabbing and plugging.

**Fig. 1.** Photograph of PVC core boxes at the loading dock of a CT Lab.

* Corresponding author: siddiqui.shameem@gmail.com

**Fig. 2**. Fiberglass core sleeve with rubber caps at the two ends placed concentrically in the Plexiglas housing of a converted medical CT-scanner before scanning.

Both medical and industrial CT-scanners can be used for whole core CT-scanning, with each one having its own advantages and disadvantages. A comparison between the two types of scanners for various petrophysical applications is presented in Ref. [1]. Industrial CT-scanners, which include the micro and nano CT-scanners, offer a wide range of X-ray voltages and intensities, and provide excellent spatial resolution, sometimes to the pore level. They are more preferred for evaluating small plugs and cuttings rather than whole cores, mainly because the scanning speed is very slow and the samples must be rotated in a vertical position during scanning, which may be detrimental to the sample integrity, especially for unconsolidated or naturally fractured cores.

Medical CT-scanners, with their large weight capacity, reasonable spatial resolution (typically 0.3 to 0.5 mm pixel length) and fast speed (especially with multi-slice technology), are ideal for scanning whole cores for various petrophysical applications. Although a properly calibrated Medical CT-scanner is capable of generating high quality images for most reservoir rocks, the data are not always sufficient for quantitative analysis that may be required for advanced petrophysical applications. In the next section, a discussion is made on the necessary modifications that would make a medical CT-scanner useful for scanning various types of reservoir rocks and for getting meaningful quantitative data for integrated reservoir studies.

## 2 CT-Scanner Modifications Needed for Petrophysical Applications

The selection of the medical scanner for petrophysical applications is of primary importance. Some of the points that should be considered during the selection process include maximum voltage, whether or not it is dual-scan capable, number of slices (for multi-slice CT-scanners), capability to do pilot scans and their lengths, etc. Medical CT-scanners are designed for human subjects and exposure of soft tissues, where maximum X-ray voltage, scanning speed are all very important considerations. Due to safety and intellectual property issues, many manufacturers are generally not willing to share advanced calibration and data transfer information with the non-medical clients and it is therefore, essential to obtain necessary permissions before purchasing a new scanner from a particular vendor. Sometimes it is more convenient to go through a third-party vendor with good connections with the CT-scanner manufacturers and good familiarity of petrophysical CT-scan requirements.

In general, modifications are needed in three major areas to convert a medical CT-scanner into one that can be used for petrophysical applications. The first one is the modification of the patient bed into a sturdier metallic table. The strong cantilever arm used to support the patent bed is not designed to align a 3 ft long core box, and since core alignment is crucial for petrophysical measurements, it is better to replace the soft patent bed with a steel table fitted with a pair of vises to ensure the proper centering of the core box or core tube. Fig. 2 shows how a vise mounted on the modified patent table (right) and another vise mounted on an added rear table are used to align a Plexiglas tube, which in turn, holds and centers the fiberglass core sleeve with the help of foamed plastic rings.

The second required modification is that of the internal calibration tables. Having the access to the calibration tables and permissions to modify them in order to scan the rocks is very important. Normally the manufacturers calibrate the scanner with a “water phantom” containing a radiopaque salt (typically sodium iodide) in water, which is sufficient for scanning human subjects. Reservoir rocks with typical grain density of 2.65 (quartz) to 2.86 (dolomite) g/cm$^3$ require calibration with solid phantoms of similar grain density, such as fused quartz, Macor, etc; it ensures artifact-free images at the different anticipated energy levels (X-ray voltage/intensity combinations). An experienced user or a designated service technician should be able to generate these calibration tables so that they can be used by the operator readily for different materials (e.g., carbonates or clastic rocks), different sizes of scanned objects (e.g., 6” diameter core box, 4.5” diameter core sleeve, 1.5” diameter core plugs, etc.), as well as for different energy levels. Every time the X-ray tube is replaced, new calibration tables must be created again.

The third modification relates to transferring data from the CT-scanner. The image processing software that are usually packaged with the CT-scanners are only good for general viewing and quality control (QC), as far as petrophysical applications are concerned. So, transferring data to workstations loaded with specialized image processing software is very important. In the past, different manufacturers used different data formats and some of them would deliberately make it difficult to track the data (due to patient data security concerns) or to transfer the data as straight files.

Today the process has mostly been streamlined and most manufacturers conform to the DICOM format, which is also readable by most of the image processing programs designed for petrophysical analysis of CT data. Many CT-scanners allow direct retrieval of data on USB drives rather than going through the network, which simplifies matters further.

## 3 Use of Calibration Standards

For whole core CT-scanning, usually the actual cores remain out of sight unless it is decided to scan bare cores, extruded from their aluminum or fiberglass sleeves. They are either devoid of any liquid or have some initial liquid saturation. Therefore, a set of calibration 'standards' is necessary to extract meaningful data such as density, porosity, etc. from the CT images. The only quantitative data that a CT-scan slice provides is the CT number (CTN or Hounsfield Units, HU) for each voxel (volume element, 3D pixel). CT number is a function of both $Z_{eff}$(Photoelectric Effect, predominant at low energies such as 80 kV) and electron density (Compton Scattering, predominant at high energies such as 140 kV). The medical CT-scanners are generally calibrated to read a value of -1000 for air and 0 for water. Wellington and Vinegar [2] suggested using 100 kV as the threshold for these two effects.

Most medical CT-scanners are limited at 150 kV as the highest voltage in order to prevent severe damage to human soft tissues and therefore, it is a common practice in petrophysical CT-scanning with a medical CT-scanner to use either 140 or 150 kV (for single energy scanning), which allows good X-ray penetration for larger whole cores such as the 4" diameter ones in their sleeves and core boxes.

In order to convert CT numbers into bulk density for the scanned cores, Wellington and Vinegar [2] proposed to use a calibration curve similar to the one in Fig. 3, using clean sandstone samples, used as 'standards' and with known measured bulk densities, from different quarries or reservoirs. This works relatively well for extruded dry cores. However, for preserved cores inside fiberglass/aluminum sleeves and/or core boxes, it is strongly recommended to scan the standards in the same 'environment' as the actual cores to avoid having to make adjustments.

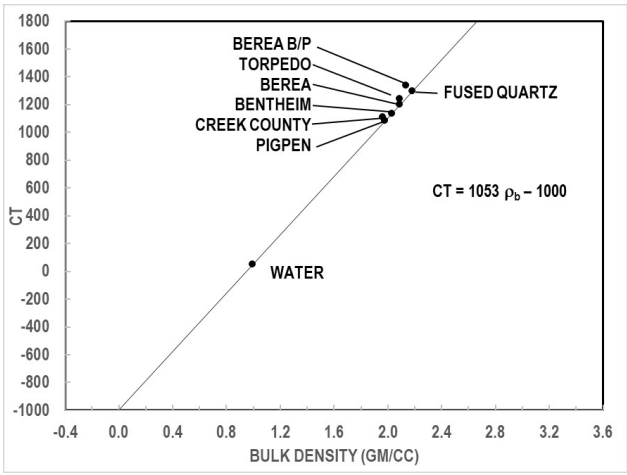


**Fig. 3.** Calibration curve of bulk density vs. CT numbers for sandstones. After Wellington and Vinegar [2].

For developed reservoirs, it is always possible to obtain bulk densities of a few cleaned (using Soxhlet extraction) representative core plugs and use them as 'standards' in addition to the solid 'standards' such as fused quartz, Macor, etc. prior to a whole core CT-scan job. Fig. 4 shows some of the 'standards' that are scanned inside the blank core sleeves prior to a whole core CT-scanning project. Scanning of these 'standards' does not take too much additional time and it should be done regularly, as these data are extremely important for conversion of CT data into bulk density.

For this case, with only one representative cleaned sandstone 'standard', the CT-derived bulk density, $(\rho_b)_{CT}$ (also called pseudo bulk density, PBD), is calculated using a straight-line relationship between CTN and $\rho_b$, for air and the representative cleaned sandstone plug, respectively. Both should be within a circular region of interest (ROI) inside the rock matrix for the core contained in the sleeve and core box, as shown in Eq. 1. Here A is the slope of the $\rho_b$ vs. CTN curve and B is the intercept.

$$(\rho_b)_{CT} = A*CTN + B \quad (1)$$

Fig. 4. Calibration 'standards' - quartz, Macor, Berea and a representative cleaned sandstone (top). Blank PVC core box and fiberglass core sleeve (bottom).

It is strongly recommended to scan multiple calibration standards each time - both solid standards and porous rock standards, although the latter group works best for converting data for reservoir rocks. In the calibration curve of $\rho_b$ vs. CTN (inverse of the graph shown in Fig. 3), it is recommended to use 0.001225 g/cm$^3$ as the density of air rather than 0, as it represents air density at room temperature and at 1 atm, at sea level. Also, there is no need to draw data for water as it may skew the data in one direction or the other. It is not recommended to mix data for carbonate and sandstone reservoir rocks in the same calibration plot. If multiple calibration standards (say, representing different facies of a clastic reservoir) are to be scanned, only data for those standards should be plotted along with the air data.

The solid 'standards' mainly help observing the drift in the X-ray tube performance, but they are usually not so good for converting CTN into $(\rho_b)_{CT}$ since they do not have any porosity. In the early days of CT-scanner use for routine and SCAL (special core analysis) evaluation of reservoir rocks, it was common to wrap small rods (about ½ inch in diameter) of different materials or tubes filled with different liquids as 'standards' around the core holder or core sleeves. Better results can be obtained by scanning solid plugs of about 1½ inch diameter placed tightly next to one another, as shown in Fig. 5, mainly because one can use a larger region of interest

(ROI) and also, the standards can be easily placed in the same environment that the actual sample is in.


Fig. 5. 1½ inch diameter calibration 'standards' placed next to one another inside a rubber sleeve for bare whole cores and plugs.

## 4 Matching CT Density Data with Logs

One of the challenges of whole core CT-scanning is matching CT based density, $(\rho_b)_{CT}$ data with bulk density log (RHOB) data. Three points should be considered for that – the first one is selection of proper calibration standards to convert the data, which is described in the previous section; the second one is fluid effect, which will be discussed below; and the third is the depth shifting issue, which will also be discussed later.

When logging is done in the wellbore, it is generally filled with mud and the adjacent formation is fully saturated with native fluids, with some degrees of invasion by the filtrate. Since the radius of investigation of density log is only about 6 inches, it mostly measures bulk density of the invaded zone, filled with a combination of fluids. When a core is sectioned at the wellsite, the difference between reservoir pressure and atmospheric pressure (except with specific pressure coring) causes a good part of the reservoir fluid contained in the pores to be expelled and replaced by air, which is harder to remove even when the sectioned core is placed with or without sleeve, capped or uncapped, inside the brine-filled core box. Leaks during the transportation and storage prior to CT-scanning may also introduce more air into the cores being scanned. So, chances are high for the scanned core to have its pore space filled with air rather than liquids. Because the conversion of CTN into $\rho_b$ (Eq. 1) involves dry calibration standards, the CT-derived bulk density, $(\rho_b)_{CT}$ is essentially a bulk density with air-filled pores. A correction must be applied to the $(\rho_b)_{CT}$ data in order to match the log-derived bulk density, $(\rho_b)_{log,}$ which, applies to liquid-filled bulk density and this is shown in Eq. 2.

$$(\rho_b)_{log} = (\rho_b)_{CT} + \phi_{CT}*(\rho_{water} - \rho_{air}) \qquad (2)$$

Here, $\rho_{water}$ and $\rho_{air}$ are the densities of water and air (in g/cm$^3$), respectively, and $\phi_{CT}$ is the porosity of the CT slice. The CT-derived porosity, $\phi_{CT,}$ can be calculated from the bulk density and matrix density, $\rho_{matrix,}$ through the relation shown in Eq. 3.

$$\phi_{CT} = (\rho_{matrix} - (\rho_b)_{log}) / (\rho_{matrix} - \rho_{water}) \qquad (3)$$

This so-called liquid correction involves an iterative process because at the initial stages of calculation, the $(\rho_b)_{log}$ is not known and therefore, must be estimated with an initial value for porosity. For matrix density the values shown in Table 1 are generally used.

**Table 1.** Matrix Density of Primary Minerals

| | Primary Mineral Name | Matrix Density, g/cm$^3$ |
|---|---|---|
| 1 | Calcite | 2.71 |
| 2 | Dolomite | 2.86 |
| 3 | Anhydrite | 2.95 |
| 4 | Quartz | 2.65 |
| 5 | Clay/Shale | 2.65 |

For the liquid correction process, it is also recommended to use tube average or facies average porosity data rather than individual slice porosity data, otherwise the calculations become very tedious, especially if large number of CT slices are involved (i.e., for thick reservoirs). The steps for this iterative process, using EXCEL, are given below:

1. Create a table with the following columns - the depth of the CT-slice, $(\rho_b)_{log}$ from Eq. 2, $\phi_{CT}$ from Eq. 3. The calculation of $(\rho_b)_{log}$ should also include A, B and the respective CTN values used in Eq. 1.
2. Create the following additional columns – average depth of the core tube, average $(\rho_b)_{log}$ for core tube and average $\phi_{CT}$ for core tube.
3. Create an additional column for average porosity containing the same value for a core tube or for certain facies. Create a last column in which the numerical data are pasted from the previous column. Note that the porosity value for liquid correction in Eq. 2 points to the very last column only.
4. For the first pass, fill up the entire last column with one initial value, say 0.15, for the entire CT-scanned interval. Because of the way the equations are set up, the second column will have an initial value of $(\rho_b)_{log}$, which will then be used to calculate a $\phi_{CT}$ for each of the slices. The second-to-last column will then get updated with a new value for each core tube (or facies, covered by several core tubes). Manually copying the entire column date and pasting the numerical value into the last column will start the second pass, and so on.
5. At the end, the data in both the second-to-last and the last columns will be the same and at that time the second column will contain the liquid-corrected $(\rho_b)_{log}$ data and the third column, the corresponding $\phi_{CT}$ data. The depths in the first column, with the CT-derived density and porosity data can then be used for comparing against logs.

If some additional slice quality control is also done to ignore the CT artifacts and missing/bad data, this workflow can produce excellent CT versus log correlations. It should be noted that typical vertical resolution of a logging tool is about 6 inches whereas multi-slice CT-scanners can take

several slices per inch, making a continuous map of CT numbers within each slice. Unless there are operational limitations for taking single scans, it is recommended to scan the whole cores at fixed intervals such as 0.5-inch, 1-inch, 2-inch, etc. This reduces the number of slices and thus, the image processing time; and the resolution is sufficient for slice-by-slice calculations for core to log comparison.

The last piece of work that needs to be done is the depth correction. It is quite common to have some mismatch between driller's depths (that all cores use) and logging depth. This causes a problem for core-log integration, core sample selection for SCAL and routine core analyses, well treatment design, etc. In typical core operations, the Core Gamma tool is used to align core depths with log depths. It works on matching the spikes seen in shale streaks in clastic rocks in both logs and cores. It generally works better if the cores are already extruded from the sleeves. For carbonate cores, which mainly contain calcite and dolomite, gamma ray variations are not very noticeable but the large density difference between calcite and dolomite makes CT a better tool for depth matching for carbonates compared to Core Gamma [2, 3]. Overall, the depth accuracy improves a lot if the depth of the top of the core in each tube is accurately known through pilot scans (also called scout scans). For scanners without the pilot scan feature, tilting the core box to move the core sleeve inside the core box to one side, prior to the CT-scans, and scanning from approximately the same position for all core boxes may result in reduction of location errors.

For dual energy CT-scanning, one of the important factors to consider is the positioning of the samples at the exact same location. Some of the most recent CT-scanners can take a high-energy scan and a low-energy scan in one single pass and for those scanners positioning is not an issue. However, in the case of older CT-scanners requiring an elaborate process for changing voltage settings for dual energy CT-scanning, the scanning must start from the same starting point and to be repeated at each slice location. Minor shifts can make the dual-energy CT-scanning analysis very difficult. It should be remembered that in order to ensure artifact-free data, appropriate calibration tables should be used for each energy and sometimes, it is more than just pushing the 140 kV or 80 kV button on the control panel.

## 5 CT Image Artifacts

Just like its medical counterpart, petrophysical CT-scanning also has to deal with several CT image artifacts during data processing. The most common ones are streaks (aliasing), ring, and beam hardening [4, 5]. Streaks appear as dark lines that radiate away from sharp corners. For the cylindrical cores this is usually not a problem as the cross section is circular. However, if the core inside the sleeve or core box is fractured naturally or during the coring process, it is possible to get sharp edges, and streaks can be observed. For the extruded, dry cores, if they are already slabbed before scanning, streaks may also be encountered from the sharp edges. Also, if core plugs are scanned in sagittal position, which presents a rectangular cross-section to the scanner, X-shaped streaks may be observed [Fig. 6]. There is hardly any post-processing correction for the streaks and during data analysis slices containing streaks should not be considered.

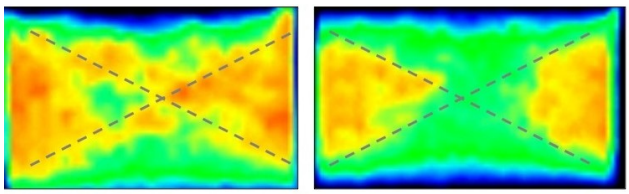

Fig. 6. Examples of X-shaped streaks in core plugs (sagittal case).

The ring artifacts, which appear as a series of off-centered concentric rings in some CT slices, are rare for medical CT-scanners, but are more common for industrial CT-scanners. It is caused by the imperfect detector elements at a specific position in the detector array. The large number of detectors used by the medical scanners as well as good centering of core samples within the CT gantry makes them rare.

The last and the most common artifact seen during whole core CT-scanning is the beam hardening artifact. The filtering of a polychromatic X-ray beam by the scanned object causes beam-hardening (cupping) artifacts. Because of beam-hardening, a perfectly homogeneous object appears to have a dense periphery. If one draws a profile on the CT slice, going from one end of the object to the other end through the center, the profile looks like a cup.

It is preferable to eliminate all the artifacts before the image is acquired through improved remedial actions and improved calibrations. In general, the medical CT-scanner calibration process with relatively large circular phantoms (having a slightly larger size than the largest object scanned) appropriate for the density range of the objects to be scanned helps minimize or eliminate this artifact.

Beam hardening is more common in bare core images rather than images of cores within core boxes and core sleeves because the polychromatic X-ray beams get pre-hardened before penetrating the rock materials. Insufficient penetration due to lower energy for large objects can also have the appearance of beam hardening on the images. In Fig. 6, the calibration was right for the vuggy carbonate core, pictured on the left, which shows no beam hardening. However, the image on the right shows strong beam hardening due to the calibration phantom not being appropriate for the material (anhydrite) in the core slice.

Beam hardening directly affects whole core CT-scanning results and forces one to use a smaller ROI, away from the edges, thus reducing the sample population for the voxels. Some image processing software include the beam hardening correction which may be used if there are no other alternatives. Since beam hardening may not be present in all the slices, the quantitative data from the beam hardening-corrected images may have some consistency issues when compared against non-corrected images.

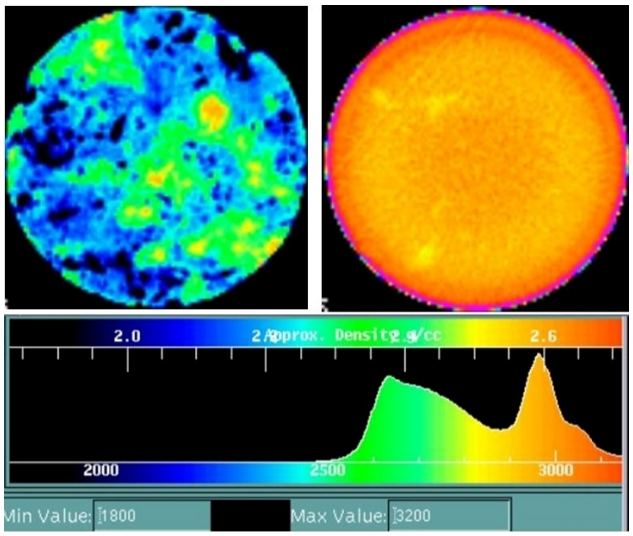


Fig. 7. Example of slices without (left) and with beam hardening (right). Histogram with overall range for all the slices scanned in the batch is shown at the bottom.

## 6 Image Processing

There are several image processing software packages, both commercial and non-commercial, for processing the CT-scan images. They are also compatible with multiple image data formats that are commonly used by the CT-scanners. Most of this software is designed for medical imaging of human subjects and may therefore not be able to cater to the need of petrophysical CT-scanning. It is not within the scope of this paper to review various software available and describe their advantages. However, some of the essential or useful features for petrophysical CT-scanning software are listed below:

1. Ability to import and read multiple image data formats generated by various manufacturers of CT-scanners. It should also be able to select multiple images at will from a group of image files.
2. Ability to digitally align the slices as it is almost impossible to have perfect alignment of slices for a core tube before scanning.
3. Ability to do ROI statistics with multiple ROI options such as circular, elliptical, polygonal, square, etc. The statistical data should include mean, minimum, maximum, standard deviation, and histograms. It should also allow drawing profiles on any slice and extract the CTN on the profile.
4. Ability to use an array calculator with functions such as add, subtract, multiply, divide, absolute, log, exponential etc., and also to apply various filters. This feature allows reporting of whole core data in terms of density or porosity units; and SCAL data in terms of saturations; rather than CTN.
5. Ability to use multiple color schemes such as grayscale, heat, rainbow, etc.; and some continuous and discrete color schemes; and the ability to create new color scales, if needed.
6. Ability to create orthogonal slabs (similar to slabbed cores), both horizontal and vertical.
7. Ability to do segmentation and thresholding.
8. Ability to generate 3D volumes (volume rendering such as iso-surface plots) from CT-slices with ability to pan, rotate, move etc.

Some of the desired advanced features specific to routine and also, SCAL type petrophysical CT-scanning should include the following:

9. Beam hardening correction.
10. Dual-energy CT calculation (Bulk density and $Z_{eff}$) using analysis like reference [6].
11. Individual fluid phase calculations using advanced image subtraction, with radiopaque solution (dopant) mixed in oil, water and gas phases.

## 7 List of Some of the Applications of Whole Core CT-scanning

CT-scanning has been used for evaluating reservoir rocks for over 35 years and many good reviews of various routine and SCAL type of applications are available in the literature [4, 7, 8 and 9]. While more and more applications are coming up, CT is currently being used for at least the following applications for the whole cores:

1. Bulk density determination: details are discussed in this paper.
2. Porosity determination from bulk density: details are discussed in this paper.
3. Quick preview of the core tubes for sample selection: Fig 8 from Ref. [11] shows density variations in CT slices taken at 2-inch intervals for 20 core tubes covering about 60 ft of a reservoir. This provides a quick preview of the condition of the preserved cores and helps in determining what samples are intact and can be used for plugging.
4. Depth matching: It is discussed in Refs. [2, 3] and Fig. 9 is taken from Ref. [10]. The images on the left are the slab images (horizontal and vertical) for five core tubes. The log data (RHOB) are shown with the red lines, the CT-derived density data (PBD) are shown with black lines, for the tube average data and with green dots, for the slices.
5. Formation damage due to mud: Fig. 10 is taken from Ref. [11] and it shows a CT slice of a 4 in diameter whole core from a sandstone reservoir. The barite-laden mud is shown to penetrate deep inside the core. The yellow outer ring is the aluminum sleeve, the bright red inner ring is the barite mud at the periphery and the dark blue material is the sandstone core. The black channels filled with mud are the fractures, possibly induced during coring. Ref. [12] has more examples of mud invasion.
6. Heterogeneity quantification and SCAL sample selection: Fig. 11, which is taken from Ref. [13], shows two types of heterogeneity that can be defined by analyzing CT-scan slices. The nine slice images at the left (inter-slice heterogeneity case) show the presence of a distinct anhydrite nodule in the last three slices. The nine slice images at the right (intraslice heterogeneity case) show large CTN variations within each slice, with relatively small

channels available for flow. Both of these plugs were determined unsuitable for SCAL tests.

7. Lithology variation: Fig. 12, which is taken from Ref. [10], is a composite image showing 19 CT-Scan slices on the left, taken 2-inch apart from each other, and representing a 3 ft section of preserved sponge core from a sandstone reservoir. The bright color in the middle is due to lithology change from sand to shale.
8. Dual-energy based mineral characterization: Fig. 13, which is taken from Ref. [6,], shows the application of dual-energy CT-scanning for mineral characterization in a carbonate reservoir. By scanning these cores at the same slice locations at 80 kV and 140 kV, respectively, it was possible to detect the streak containing dolomites. Dual energy CT is also discussed in Ref. 14.
9. CT density-based FMI type logs: Fig. 14, taken from Refs. [15, 10] shows how CT-slice image data can be used to generate density-based FMI-type images. The example image, shown in the rightmost panel, was created by combining continuous CT-scan data for a 34 ft section of core through a process of collecting the surface slice data and unrolling them. The cores were depth-shifted prior to placing next to the FMI logs.
10. Fracture Characterization: Fig. 15, which is taken from Ref. [10] shows a 360-degree core photograph next to a CT-generated unrolled image of a fractured core that was also plugged. The CT image displays the fracture with dark blue lines, and it also shows additional fractures not visible on the surface.

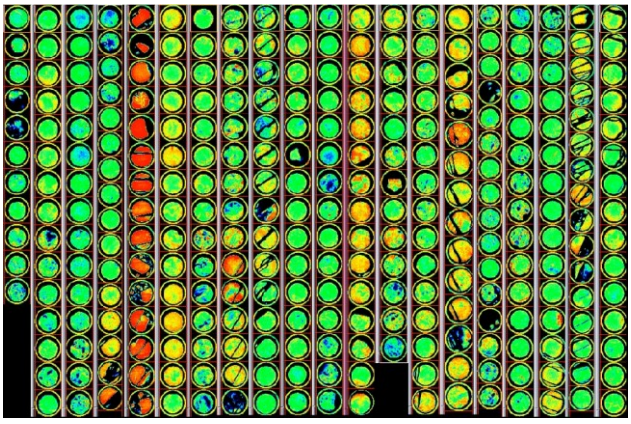

Fig. 8. Example of quick preview of the condition of the preserved cores.

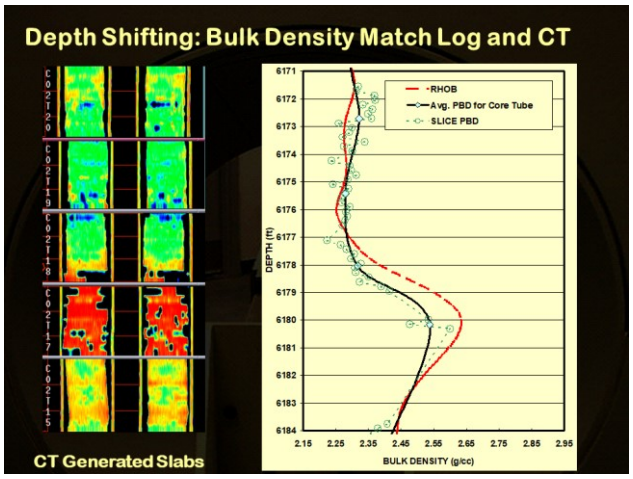


Fig. 9. Example showing how CT generated density data are used for depth shifting in a 15-ft section of a carbonate core.

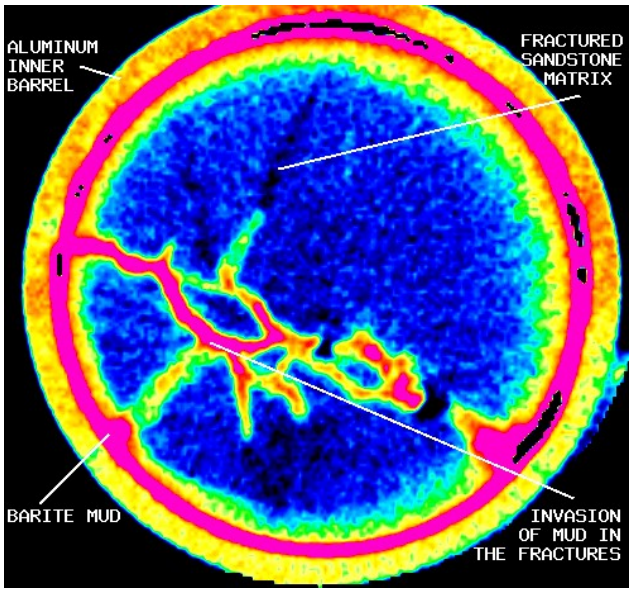


Fig. 10. Example of mud invasion in a core during the coring process.

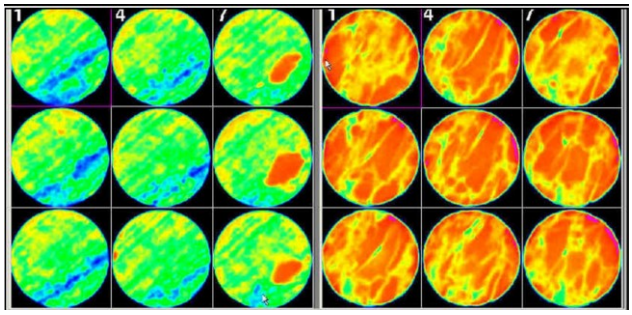

Fig. 11. CT-Scan slices for two core plugs showing case of inter-slice heterogeneity (left images), and intra-slice heterogeneity (right images).

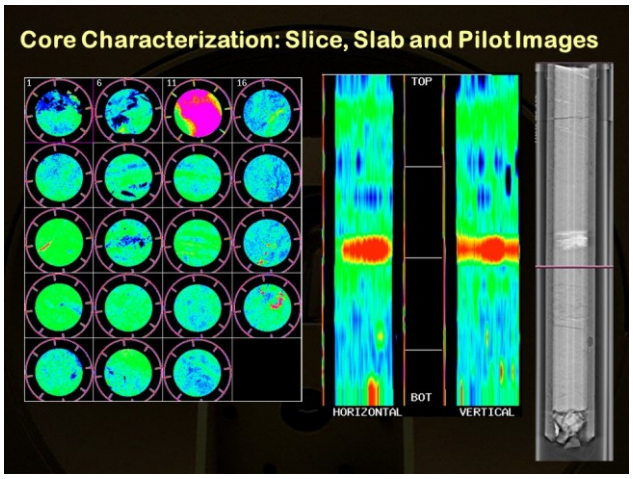


Fig. 12. Example of lithology variation within a core tube.

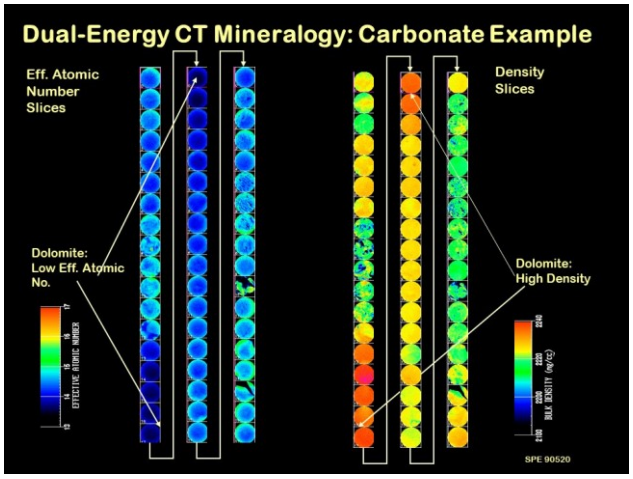


Fig. 13. Example of dual-energy based mineralogy determination using CT-Scan slices for three core tubes taken from a carbonate reservoir containing both calcite and dolomite.

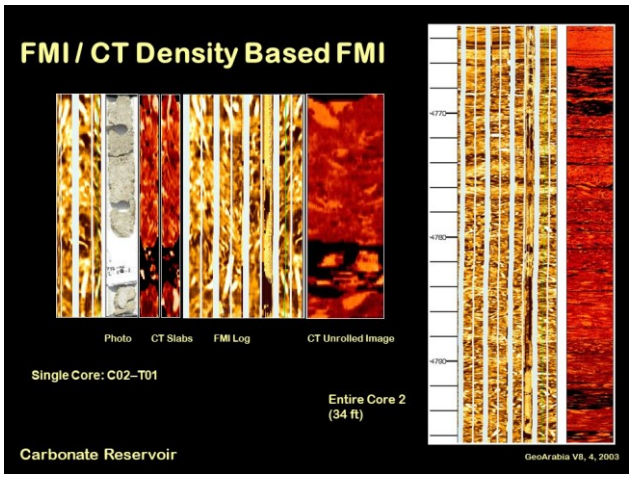


Fig. 14. Example of CT-generated density-based FMI (formation micro imager log) type images (rightmost panel).

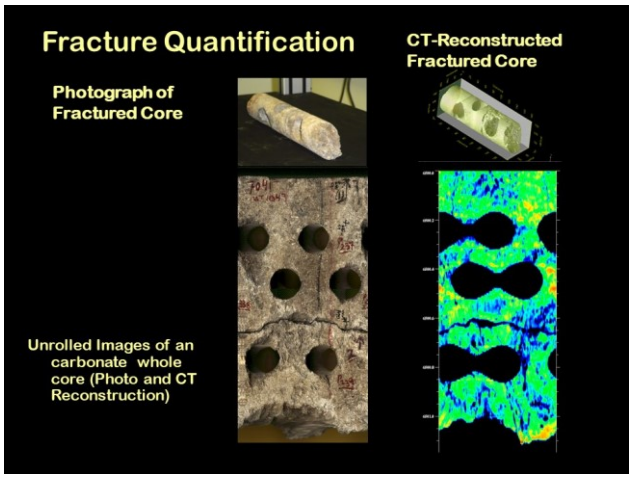


Fig. 15. Example of fracture characterization in whole cores.

## 8 Conclusions

In this paper an attempt has been made to present some of the interesting applications of computerized tomography (CT) for evaluating whole cores. Starting with what changes are needed to convert a purely medical CT-scanner into one that can generate artifact-free images of reservoir rock samples, this paper covers discussions on calibration standards and how they can be used to generate bulk density and porosity data. Step-by-step instructions on how to use an iterative approach to correct for liquid effects for matching the CT-derived bulk density and porosity data with the logs, are also provided.

This paper covers some common CT artifacts that may be encountered while using a medical CT-scanner for whole core CT-scanning. Necessary features for the petrophysical use of a CT image analysis software are also discussed. Finally, a list of ten specific applications applicable to whole core CT-scanning, with examples and references, is presented with the hope that more and more new applications of this very useful non-destructive imaging technology will be developed by the future petroleum engineers and geoscientists in order to broaden our understanding of the reservoir rocks.

## 9 Acknowledgments

The author expresses his deep appreciation for his mentors Abraham Grader, Paul Hicks and Phillip Halleck for their help and support. The author also thanks his former colleagues at the Saudi Aramco R&D Center in Dhahran, KSA, who made it possible to explore new ideas. The author appreciates the support of Bob Kehl of Kehlco, Inc. for his *VoxelCalc* petrophysical image processing software, which was used for generating some of the images.

## Nomenclature

| | |
|---|---|
| $Z_{eff}$ | Effective Atomic Number |
| CTN | CT Number |
| RHOB | Log-derived bulk density, g/cm$^3$ |
| $(\rho_b)_{log}$ | Log-derived bulk density, g/cm$^3$ |
| A, B | Slope and intercept of $\rho_b$ vs. CTN graph |
| $(\rho_b)_{CT}$ | CT-derived bulk density, g/cm$^3$ |
| $(\phi)_{CT}$ | CT-derived porosity, fraction |
| $\rho_{matrix}$ | Matrix (grain) density, g/cm$^3$ |
| $\rho_{air}$ | Air density, g/cm$^3$ |

## References

1. M.R.H. Sarker and S. Siddiqui. “Advances in Micro-CT Based Evaluation of Reservoir Rocks.” Paper presented at the SPE Saudi Arabia Section Technical Symposium, Al-Khobar, Saudi Arabia, May 2009. doi: https://doi.org/10.2118/126039-MS
2. S.L. Wellington and H.J. Vinegar. “X-Ray Computerized Tomography.” JPT, August 1987, p. 885.
3. S. Siddiqui. “Method for depth-matching using computerized tomography.” US Patent number: 6876721, 2003.
4. S. Akin, and A. R. Kovscek. “Computed tomography in petroleum engineering research.” In Applications of X-ray computed tomography in the geosciences, F. Mees; R. Swennen; M. Van Geet; P. Jacobs (Eds.), Jan. 2003. doi: https://doi.org/10.1144/GSL.SP.2003.215.01.01.
5. R.P. Kehl and S Siddiqui. “Two Less-Used Applications of Petrophysical CT-Scanning.” in Advances in Computed Tomography for Geomaterials: GeoX 2010, pp.180-188.doi: https://doi.org/10.1002/9781118557723.ch22.
6. S. Siddiqui, S. and A.A. Khamees. “Dual-Energy CT-Scanning Applications in Rock Characterization.”" Paper presented at the SPE Annual Technical Conference and Exhibition, Houston, Texas, September 2004. doi: https://doi.org/10.2118/90520-MS.
7. E.M. Withjack, C. Devier, and G. Michael. “The Role of X-Ray Computed Tomography in Core Analysis.” Paper presented at the SPE Western Regional/AAPG Pacific Section Joint Meeting, Long Beach, California, May 2003. doi: https://doi.org/10.2118/83467-MS.
8. E.M. Withjack. “Computed Tomography for Rock-Property Determination and Fluid-Flow Visualization.” SPE Formation Evaluation, December, 1988, p. 696.
9. A. Kantzas, “Investigation of Physical Properties of Porous Rocks and Fluid Flow Phenomena in Porous Media Using Computer Assisted Tomography.” In Situ, Vol. 14, No. 1, 1990, p. 77.
10. S. Siddiqui, “Understanding Reservoir Rocks through Computerized Tomography (CT) Imaging.” SPE Distinguished Lecturer Presentation, Society of Petroleum Engineers, 2013-14.
11. S. Siddiqui, “Application of Computerized Tomography in Core Analysis at Saudi Aramco.” Saudi Aramco Journal of Technology, Winter 2001, pp. 2-14.
12. H.J. Vinegar and S.L. Wellington. “Method of Determining Drilling Fluid Invasion.” US Patent No. 4540882A, 1983.
13. S. Siddiqui, T.M. Okasha, J.J. Funk, and A.M. Al-Harbi. “Improvements in the selection criteria for the representative special core analysis samples.” SPEREE 9, **06** (2006), pp. 647-653.
14. J.G.C. Coenen, and J.G. Maas. “Material Classification by Dual-Energy Computerized X-ray Tomography.” Proceedings of the International Symposium on Computerized Tomography for Industrial Applications, Berlin, Germany, 1994, pp. 120–127.
15. G.W.G. Hughes, S. Siddiqui, and R.K. Sadler. “Shu’aiba rudist taphonomy using computerised tomography and image logs, Shaybah field, Saudi Arabia.” GeoArabia 8, **4**, pp. 585-596.